Hyperscaling violating black hole solutions and transports of quantum critical points

Xian-Hui Ge

Department of Physics, Shanghai University

XHG, Yunseok Seo, SangJin Sin, Geunho Song, JHEP, 06 (2020) 018 [arXiv: 1912.12603]
Z.-N. Chen, X.-H. Ge, S.-Y. Wu, G.-H. Yang and H.-S. Zhang, *Nucl. Phys.* **B 924** (2017) 387 [arXiv:1709.08428]
XHG, Y. Tian, S.-Y. Wu and S.-F. Wu, *Phys. Rev.* **D 96** (2017) 046015 [arXiv:1606.05959]

Outline

- Introduction and motivation

  Magnetic gap of Mn-doped Bi_2Te_3

  Dirac materials

  non-Dirac materials
- Warm up: hyperscaling violating black holes without magnetic impurity
- Black hole solution with a hyperscaling violating factor and magnetic impurity
- Quantum transports and (z,θ) space
- Conclusion and outlook

1. Introduction and Motivation

- Dirac materials : graphene and topological insulator's surface has a Dirac cone

✓ Transport anomaly in graphene demonstrated that a system known to be weakly interacting may become strongly correlated if the Fermi surface is small enough.

✓ The fundamental reason for the appearance of the strong interaction in graphene is the smallness of the Fermi sea

✓ Surface of TI: weak anti-localization, quantized anomalous Hall effect, Majorana fermion and topological magneto-electric effect.

$$\alpha_{eff} = \frac{e^2}{4\pi\epsilon\hbar c}\,\frac{c}{v_F} \sim 2.2/\epsilon_r$$

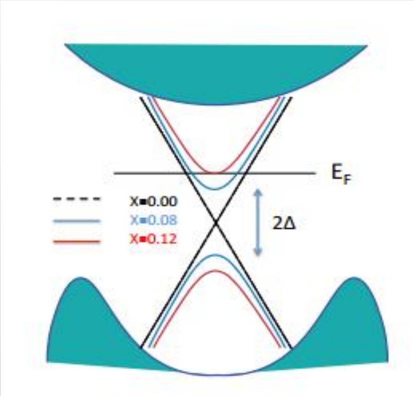

(a) surface gap of TI

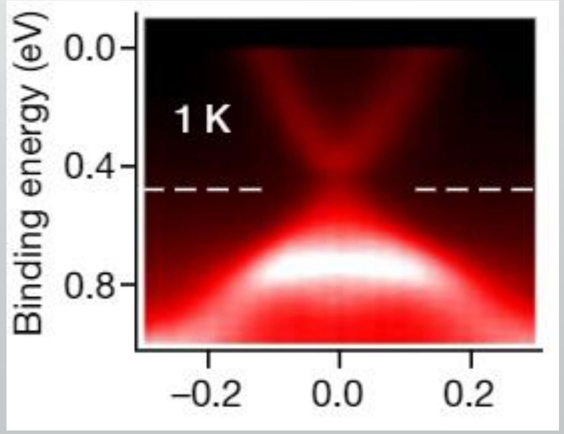

Magnetic gap of Mn-doped Bi_2Te_3

E.D. Rienks et al, nature (2019) 423

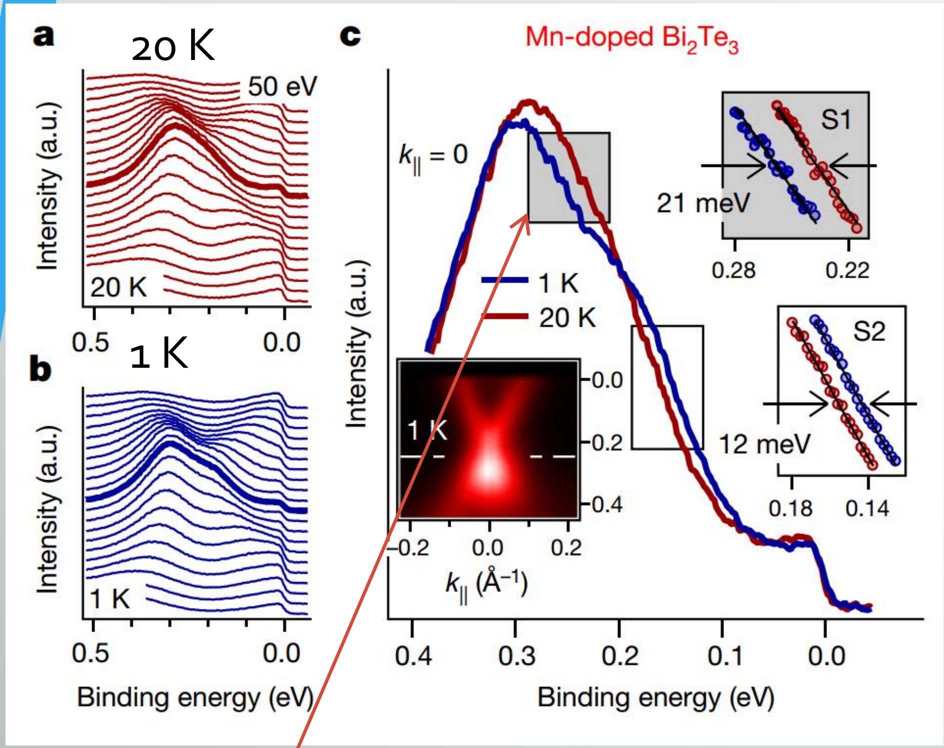

The topological surface state at 20K becomes split into two equally intense components.

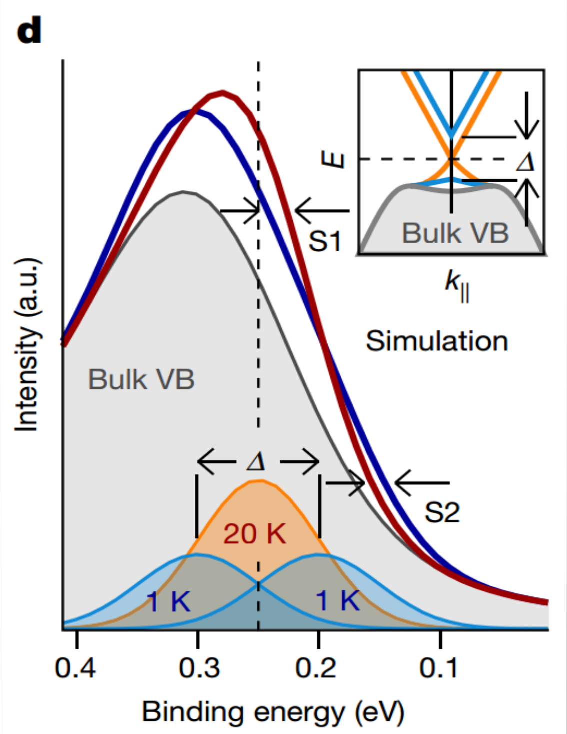

The magnetic origin of this gap. Ferromagnetic phase transition Tc=10K

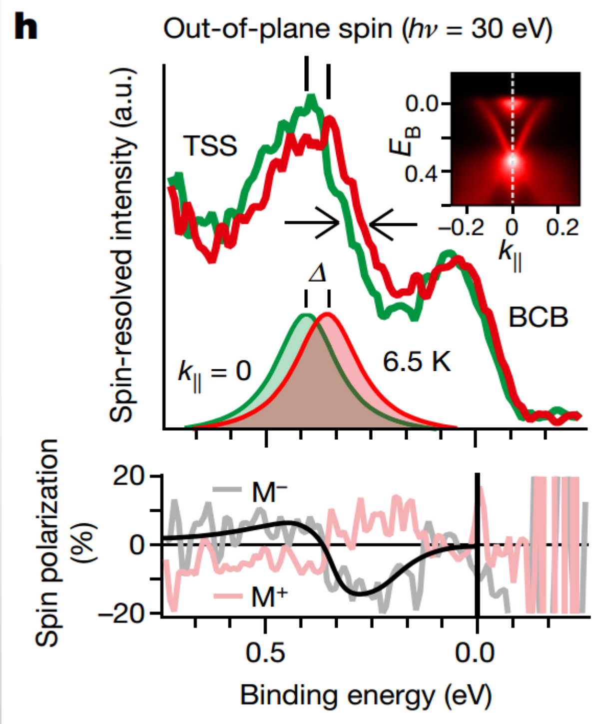

Spin-resolved ARPES. At 6.5K, the spectrum at the Dirac point is clearly spin-polarized.

Hyperscaling violating factor

- A quantum critical point is characterized by z and theta from the dispersion relation $\omega \sim k^z$ and entropy $s \sim T^{(d-\theta)/z}$
- The metric yields the same scaling symmetry

$$ds^2 = r^{-\theta}\left(-r^{2z}f(r)dt^2 + \frac{dr^2}{r^2 f(r)} + r^2(dx^2 + dy^2)\right),$$

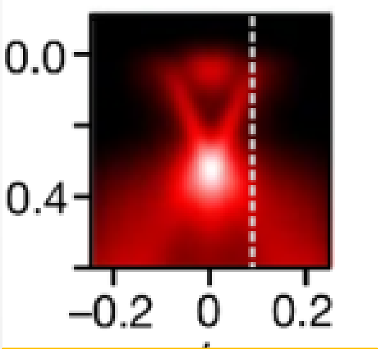

ARPES data for Mn-doped Bi_2Te_3

- Why hyperscaling violation?
- Dirac material with z=1, θ=0 agreeing with experimental data of surface of TI
- Deviation from Dirac point z=1.5, θ=1 agreeing with experimental data of Mn doped Bi_2Se_3

Non Dirac materials

- As the surface of TI is doped with the magnetic impurities, the Fermi surface becomes smaller and the surface gap is open.
- Dirac cone disappears and the system is strongly interacting when the surface band touches the Fermi level.
- The qualitative difference of the transports closely depends on the dynamical exponent of quantum critical point via various (z,θ).

We consider transport coefficients with hyperscaling violation and magnetic impurity from holography.

Notations: We focus on the consequence of the Dirac cone and surface gap of TI rather than the cause of Dirac cone and surface state of TI.
We confine our attention to the surface.

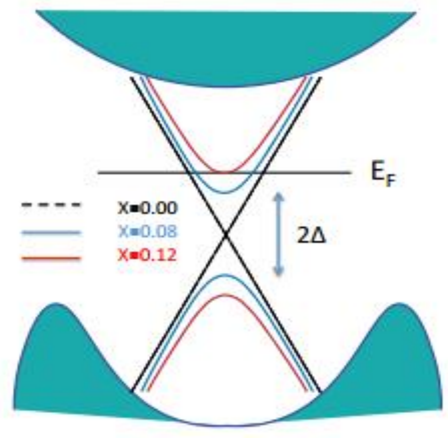

(a) surface gap of TI

2. Black hole solutions

- The model

$$S_{\rm tot} = \int_{\mathcal{M}} d^4x \, (\mathcal{L}_0 + \mathcal{L}_{\rm int})$$

potential
dilaton
Maxwell field
Linear axions:
translational symmetry broken

$$\mathcal{L}_0 = \sqrt{-g}\left(R + \sum_{i=1}^{2} V_i e^{\gamma_i \phi} - \frac{1}{2}(\partial\phi)^2 - \frac{1}{4}\sum_{i=1}^{2} Z_i(\phi) F_{(i)}^2 - \frac{1}{2} Y(\phi) \sum_{i,I}^{2} (\partial \chi_I^i)^2\right)$$

$$\mathcal{L}_{\rm int} = -\frac{q_\chi}{16} \sum_{I=1,2} (\partial\chi_I^{(2)})^2 \epsilon^{\mu\nu\rho\sigma} F^{(2)}_{\mu\nu} F^{(2)}_{\rho\sigma},$$

$$Z_i = e^{\lambda_i \phi}, \quad Y(\phi) = e^{-\lambda_2 \phi}, \quad \chi_i^I = \beta^I \delta_{Ii} x^i,$$

Magnetic impurity

- The black brae solution

Auxiliary gauge field

Maxwell fields

$$A_1 = a_1(r)dt, \qquad A_2 = a_2(r)dt + \frac{1}{2}H(xdy - ydx),$$

$$\chi_I^{(1)} = (\alpha x, \alpha y), \qquad \chi_I^{(2)} = (\lambda x, \lambda y),$$

$$ds^2 = r^{-\theta}\left(-r^{2z} f(r) dt^2 + \frac{dr^2}{r^2 f(r)} + r^2(dx^2 + dy^2)\right),$$

$$f(r) = 1 - m r^{\theta - z - 2} - \frac{\beta^2}{(\theta-2)(z-2)} r^{\theta - 2z} + \frac{q_2^2(\theta - z) r^{2\theta - 2z - 2}}{2(\theta - 2)}$$

$$+ \frac{H^2 r^{2z-6}}{4(z-2)(3z-\theta-4)} + \frac{\lambda^4 H^2 q_\chi^2 c_3}{r^{6+2z-4\theta}} - \frac{\lambda^2 H q_2 q_\chi c_2}{r^{4+2z-3\theta}},$$

magnetic impurity term

$$a_1(r) = \frac{-q_1}{2 + z - \theta}(r_{\rm H}^{2+z-\theta} - r^{2+z-\theta}), \quad a_2(r) = (\mu - q_2 r^{\theta - z}) - \frac{\lambda^2 H q_\chi c_4}{r^{z - 2\theta + 2}},$$

As z->1, theta->0, we recover the result given in Y. Seo, G. Song, C. Park and S. J. Sin, JHEP 1708.02257

Warm up: black hole solution with q_χ=0

- Two branches of black hole solution: first branch

$$f = 1 + \frac{(q_2)^2 r^{2\theta-2z-2}}{2(\theta-2)(\theta-z)} + \frac{B^2 r^{2z-6}}{4(z-2)(3z-\theta-4)} - \frac{k^2 r^{\theta-2z}}{(\theta-2)(z-2)} - m r^{\theta-z-2}.$$

$$\lambda_2 = \frac{\beta}{2-\theta}, \quad \eta = \frac{\beta}{\theta-2}, \quad \lambda_1 = \frac{\theta-4}{\beta}, \quad \gamma_2 = \frac{\theta+2z-6}{\beta},$$

$$(q_1)^2 = \frac{2V_1(z-1)}{z-\theta+1}, \quad V_2 = \frac{B^2(2z-\theta-2)}{4(z-2)}.$$

Hawking temperature

$$T = \frac{1}{4\pi}\left[(z-\theta+2)r_+^z + \frac{(q_2)^2 r_+^{2\theta-z-2}}{2(\theta-2)} + \frac{B^2 r_+^{3z-6}}{4(z-2)} + \frac{k^2 r_+^{\theta-z}}{\theta-2}\right].$$

- Second branch

$$f^* = 1 + \frac{(q_2)^2 r^{2z-6}}{4(z-2)(3z-\theta-4)} + \frac{B^2 r^{2\theta-2z-2}}{2(\theta-2)(\theta-z)} - \frac{k^2 r^{\theta-2z}}{(\theta-2)(z-2)} - m r^{\theta-z-2}.$$

$$\lambda_2^* = \frac{\beta}{\theta-2}, \quad \gamma_2^* = \frac{\theta+2z-6}{\beta}, \quad V_2^* = \frac{(q_2)^2(2z-\theta-2)}{4(z-2)}.$$

Hawking temperature

$$T^* = \frac{1}{4\pi}[(z-\theta+2)r_+^z + \frac{(q_2)^2 r_+^{3z-6}}{4(z-2)} + \frac{B^2 r_+^{2\theta-z-2}}{2(\theta-2)} + \frac{k^2 r_+^{\theta-z}}{\theta-2}].$$

Magneto-thermoelectric DC conductivities

- Lifshitz spacetime with two gauge fields : one auxiliary field and one gauge field
- The mixture of the two gauge fluctuations leads to a 2x2 conductivity matrix with non-vanishing off-diagonal components
- To avoid ambiguities, we set the currents induced by the auxiliary gauge field to be vanishing so that the deduced conductivity matrix is only related to the black hole charges
- Even in the absence of linear axions, finite DC conductivity can be obtained for finite q1 and q2 without momentum dissipation

Finite conductivity without momentum dissipation

- The resulting thermoelectric conductivities

$$\sigma_{xx}=\sigma_{yy}=\frac{q_1^2[Z_1(q_2^2+Z_2^2B^2)+Z_2(q_1^2)]}{[q_1^2+Z_1(Z_2B^2)]^2+Z_1^2q_2^2B^2},$$

$$\sigma_{xy}=-\sigma_{yx}=\frac{Z_1q_2B[Z_1(q_2^2+Z_2^2B^2)+2Z_2(q_1^2)]}{[q_1^2+Z_1(Z_2B^2)]^2+Z_1^2q_2^2B^2},$$

$$\alpha_{xx}=\alpha_{yy}=\frac{4\pi Z_1Wq_2q_1^2}{[q_1^2+Z_1Z_2B^2]^2+Z_1^2q_2^2B^2},$$

$$\alpha_{xy}=-\alpha_{yx}=\frac{Z_1q_2B[Z_1(q_2^2+Z_2^2B^2)+2Z_2q_1^2]}{[q_1^2+Z_1Z_2B^2]^2+Z_1^2q_2^2B^2}.$$

- In the absence of magnetic field, namely B=0, the electrical conductivities reduces to

$$\sigma_{xx}=\sigma_{yy}=Z_2+\frac{q_2^2Z_1}{q_1^2},\ \sigma_{xy}=\sigma_{yx}=0.$$

- Linear resistivity: **$\theta=8/5$, $z=6/5$ for the first branch of solution**
  θ=0, z=2 for the second branch of solution

Nernst signal as a functions of B and T

$\theta = -1, z = 1$ for the second branch of solution

$\theta = 8/5, z = 6/5$ for the first branch of solution

θ=0, z=2 for the second branch of solution

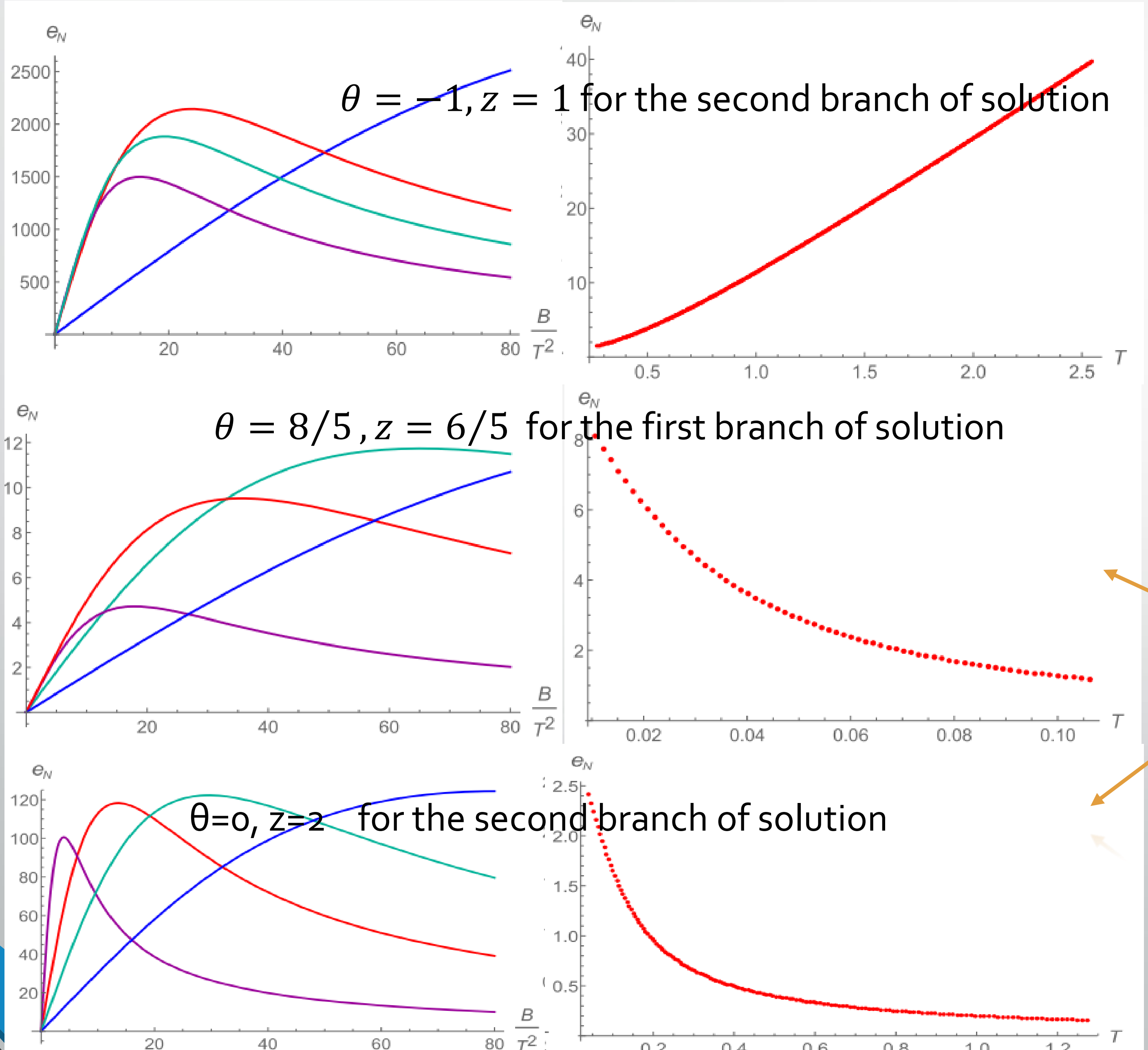

Without momentum dissipation

Classification of (z,θ) space

- The entropy density and the Hawking temperature

$$s = 4\pi r_H^{2-\theta}$$

$$T = (z+2-\theta)\, r_H^{z} - \frac{\beta^2}{2-\theta}\, r_H^{\theta-z}\, (\theta H - (z-\theta)\, q2)^2 - \frac{H^2 r_H^{3z-6}}{4\,(z-2)}$$

- Near horizon geometry $AdS_2 * S^2$

$$ds^2 = \frac{-d\tau^2 + du^2}{l_{\rm eff}^2 u^2} + r_{\rm H}^{2-\theta}(dx^2 + dy^2).$$

Hawking-Page phase transition?

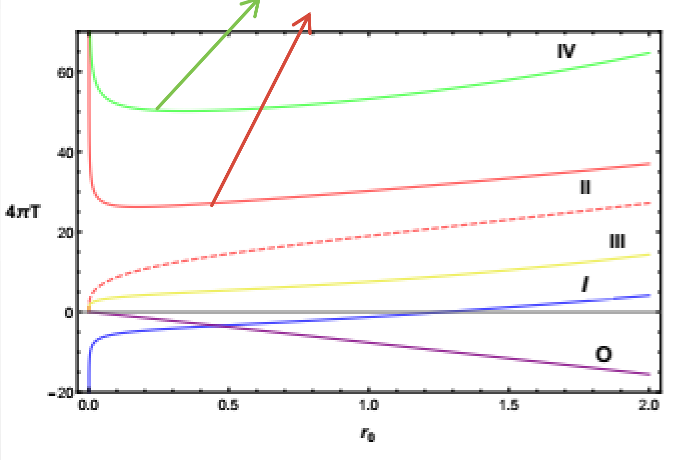

(b) r_0 vs T

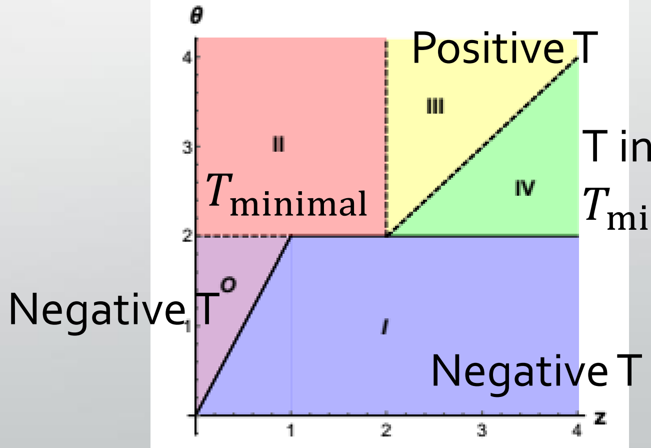

(a) Classification of (z, θ) space

3. Magneto-transport with magnetic impurity

- Linear response perturbations

$$\delta g_{tx} = h_{tx}(r) + t f_{3x}(r), \quad \delta g_{ty} = h_{ty}(r) + t f_{3y}(r), \quad \delta g_{rx} = h_{rx}(r), \quad \delta g_{ry} = h_{ry}(r),$$
$$\delta A_{ax} = b_{ax} - t f_{ax}, \quad \delta A_{ay} = b_{ay} - t f_{ay}, \quad \delta\chi_1 = \varphi_x(r), \quad \delta\chi_2 = \varphi_y(r).$$

- The transport coefficients

$$\sigma_{ii} = \frac{Z_2\left(\mathcal{F} + Y\mathcal{G}^2\right)\left(\mathcal{F} - Z_2 H^2\right)}{\left(\mathcal{F}^2 + H^2\mathcal{G}^2\right)},$$
$$\sigma_{ij} = \epsilon_{ij}\left(\Theta + \frac{Z_2 H\mathcal{G}\left(2\mathcal{F} + Y\mathcal{G}^2 - Z_2 H^2\right)}{\left(\mathcal{F}^2 + H^2\mathcal{G}^2\right)}\right),$$
$$\alpha_{ii} = \bar{\alpha}_{ii} = \frac{s\mathcal{G}\left(\mathcal{F} - Z_2 H^2\right)}{\left(\mathcal{F}^2 + H^2\mathcal{G}^2\right)},$$
$$\alpha_{ij} = \bar{\alpha}_{ij} = \epsilon_{ij}\frac{sH\left(Z_2\mathcal{F} + \mathcal{G}^2\right)}{\left(\mathcal{F}^2 + H^2\mathcal{G}^2\right)},$$
$$\bar{\kappa}_{ii} = \frac{s^2 T\mathcal{F}}{\left(\mathcal{F}^2 + H^2\mathcal{G}^2\right)}, \qquad \Theta = \lambda^2 q_\chi / r_{\mathrm{H}}^{2-\theta}.$$
$$\bar{\kappa}_{ij} = \epsilon_{ij}\frac{s^2 T\mathcal{G}}{\left(\mathcal{F}^2 + H^2\mathcal{G}^2\right)},$$

$$\mathcal{F} = WY\beta^2 + Z_2 H^2 - q_2 Y\Theta H + Y\Theta^2 H^2$$
$$\mathcal{G} = q_2 - \Theta H$$

Conductivity matrix

$$\rho_{xx} = \frac{\sigma_{xx}}{\sigma_{xx}^2 + \sigma_{xy}^2}$$
$$\rho_{yx} = \frac{\sigma_{xy}}{\sigma_{xx}^2 + \sigma_{xy}^2}$$

Thermal conductivity

$$\kappa_{ij} = \bar{\kappa}_{ij} - T(\bar{\alpha}\cdot\sigma^{-1}\alpha)_{ij},$$
$$\kappa_{xx} = \mathcal{K}_{xx}/\mathcal{D}, \qquad \kappa_{yx} = \mathcal{K}_{yx}/\mathcal{D},$$

Seebeck coefficient and Nernst signal

$$S = (\sigma^{-1}\cdot\alpha)_{xx} = \mathcal{S}/\mathcal{D},$$
$$N = (\sigma^{-1}\cdot\alpha)_{yx} = \mathcal{N}/\mathcal{D},$$

$$\mathcal{S} = s(Z_2\mathcal{F} + \mathcal{G}^2)(\mathcal{G} + H\Theta),$$
$$\mathcal{N} = s(\mathcal{F} - Z_2 H^2)(\mathcal{G}\Theta - Z_2^2 H).$$

Phases of transports

Z=2, θ=2 is the singularity of the metric function

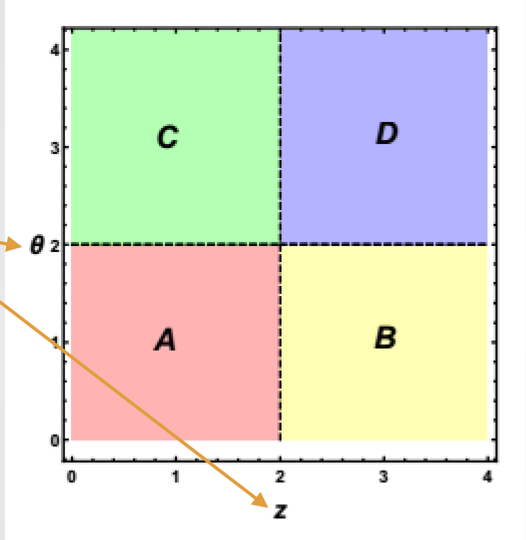

(a) Phases of transports

θ

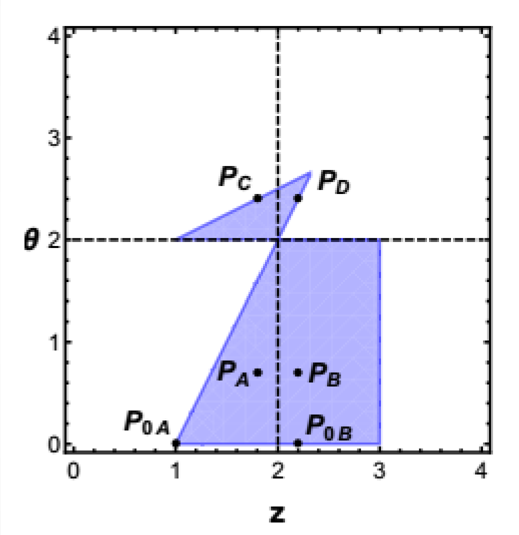

(b) Validity regime

1. The reality condition of q1 requires: (2z-2)(2+z-θ)>=0
2. Null energy condition (2-θ)(2z-2-θ)>=0

Magneto-transports vs quantum critical points

Magneto-conductivity in (z,θ) plane

- Weak anti-localization—weak localization phase transition

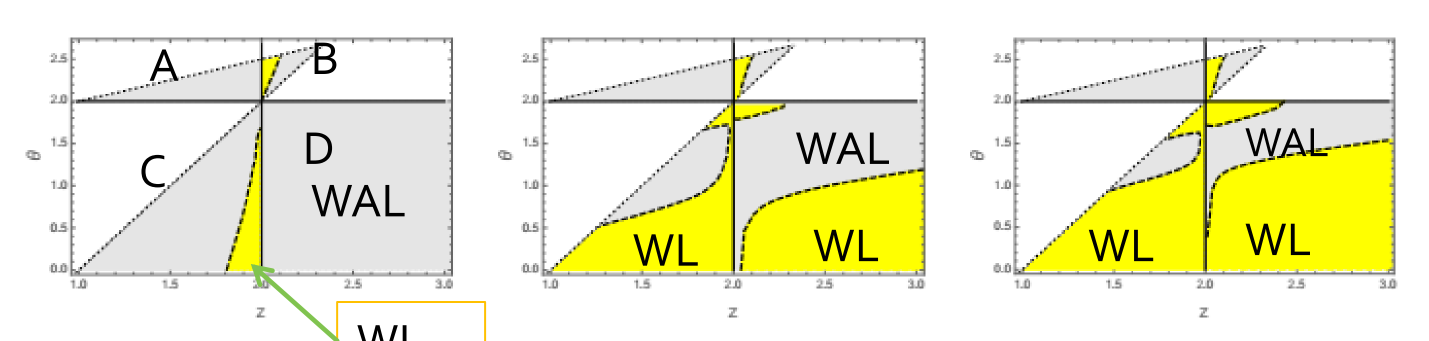

(a) $q_x = 0$ (b) $q_x = 0.7$ (c) $q_x = 1.4$

- Small H expansion of σ_{xx}

$$\sigma_{xx} = \sigma_{xx}^0 - \frac{r_0^{2z-2\theta-8}}{2}\left[\frac{2r_0^{4z}}{\beta^2} - \mathcal{A}_1(2z-\theta-2)r_0^{\theta+5} - \frac{2q_\chi^2\lambda^4 r_0^{4\theta}(1+z-2\theta)^2}{\beta^2(2+z-2\theta)^2}\right]H^2 + \cdots .$$

Weak anti-localization (WAL) for minus sign
Weak localization (WL) for positive sign

- In the absence of qx, most part of validity regime starts with WAL phase.
- As qx increases, the region of WL expands .
- As temperature increases, yellow regions in A,B shrink while yellow regions in C,D expand and fill the whole region of C,D.

σ_{xx} for different (z,θ)

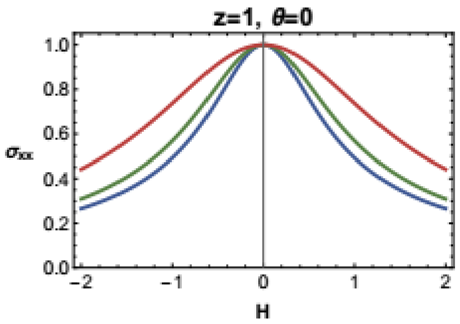

(a) P_{0A} at $q_X = 0$

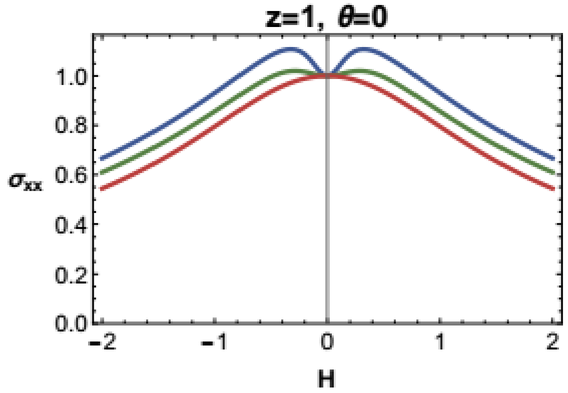

(b) P_{0A} at $q_X = 0.7$

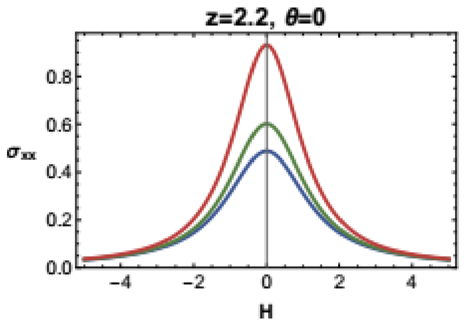

(c) P_{0B} at $q_X = 0$

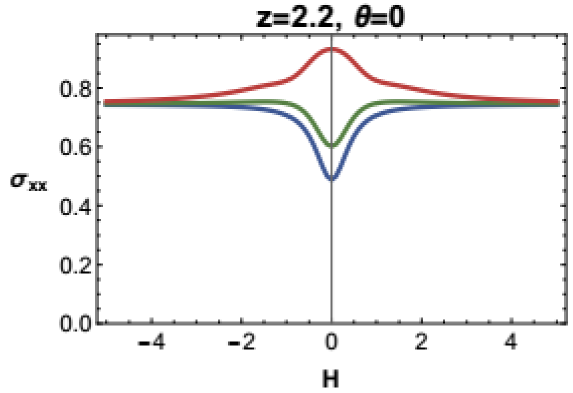

(d) P_{0B}

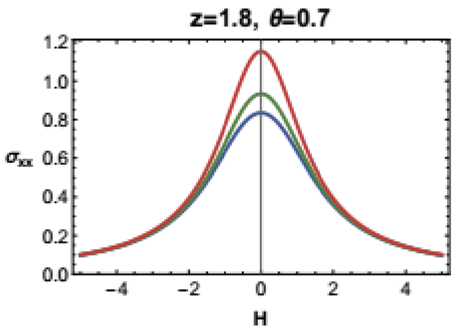

(e) P_A at $q_X = 0$

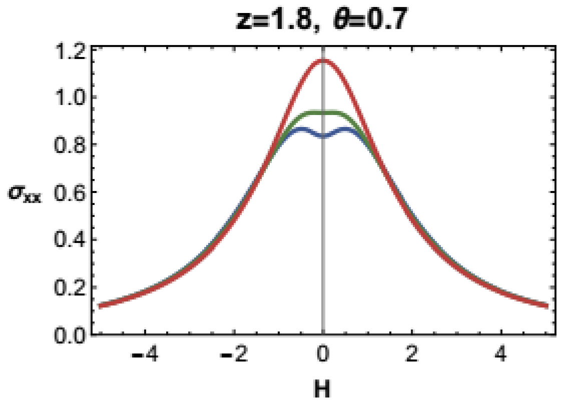

(f) P_A

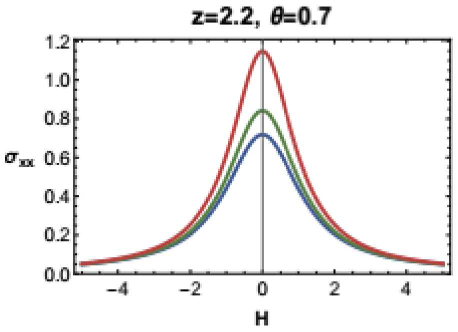

(g) P_B at $q_X = 0$

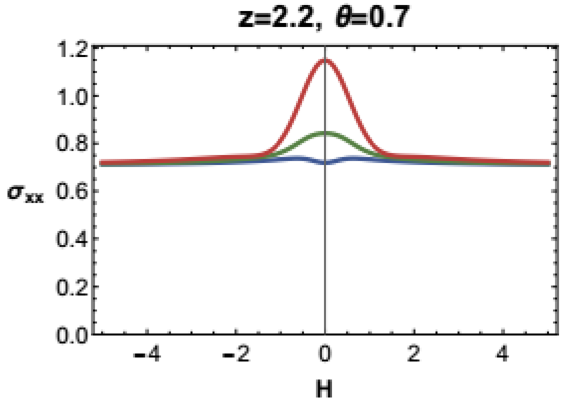

(h) P_B

Magneto-thermal conductivity in (z,θ) plane

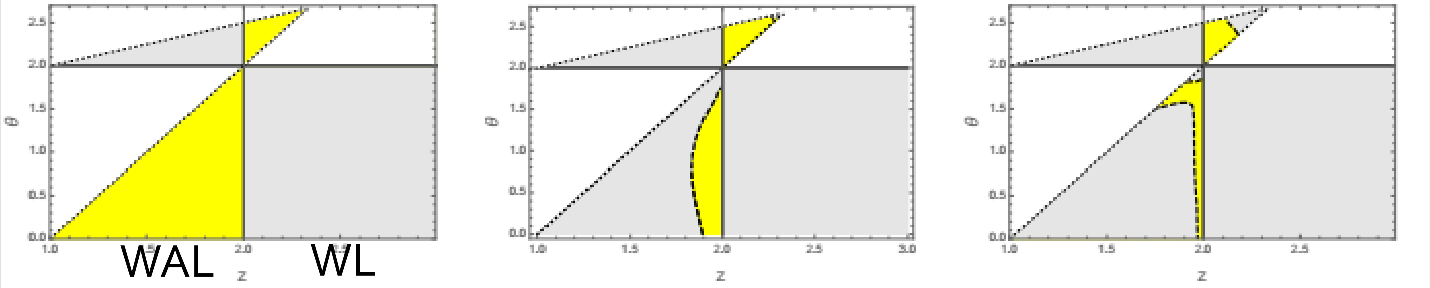

(a) $q_x = 0$ (b) $q_x = 0.7$ (c) $q_x = 1.4$

$$\kappa_{xx} = \kappa_{xx}^{0} - \frac{16\pi^2 r_0^{2z-2\theta-6} T}{\beta^4}\left[r_0^5 \beta^2 (\theta - z)\mathcal{A}_1 + \mathcal{B}_1\right] H^2 \cdots ,$$

$$\kappa_{xy} = -\frac{16\pi^2 q_x \lambda^2 r_0^{4z-\theta-6}}{\beta^4}\left[\frac{(2+z-2\theta) r_0^{4z} + q_x^2 \lambda^4 (1+z-2\theta) r_0^{4\theta}}{(2+z-2\theta)^2 (r_0^{4z} + q_x^2 \lambda^4 r_0^{4\theta})}\right] H^2 + \cdots .$$

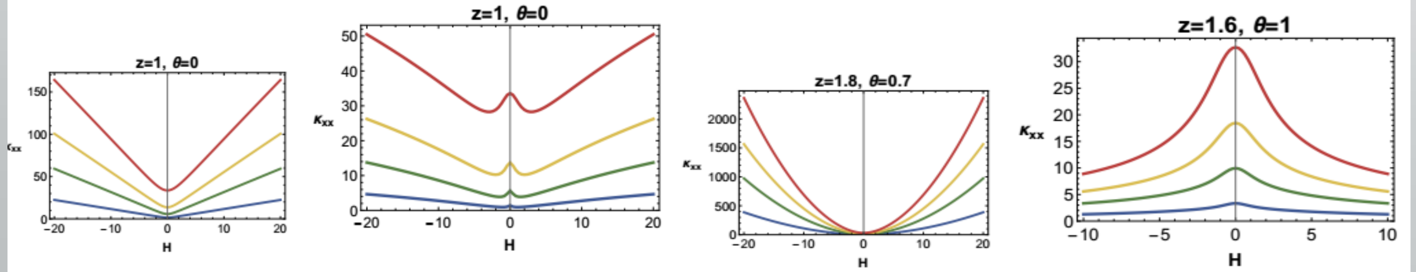

(a) P_{0A} at $q_x = 0$ (b) P_{0A} (e) P_A at $q_x = 0$ (f) P_A

- For longitudinal thermal conductivity , the sign of the coefficient is positive near z=2 and negative in other regions.
- For transverse thermal conductivity, when qx=0, the sign of coefficient is only depends on the sign of –(2+z- θ) because all other terms are positive.

Magnetically doped surface state of TI: fitting with experimental data

The best fit comes from (z,θ) =(3/2,1)

$$\Delta\sigma_{xx} = \sigma_{xx}(H) - \sigma_{xx}(0)$$

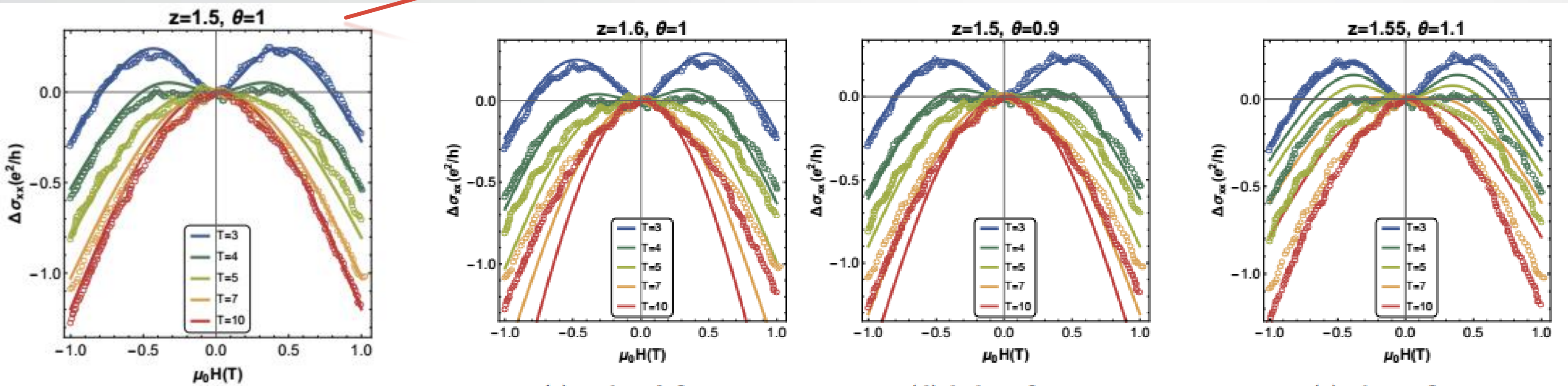

(b) At Q_2 (c) right of Q_2 (d) below Q_2 (e) above Q_2

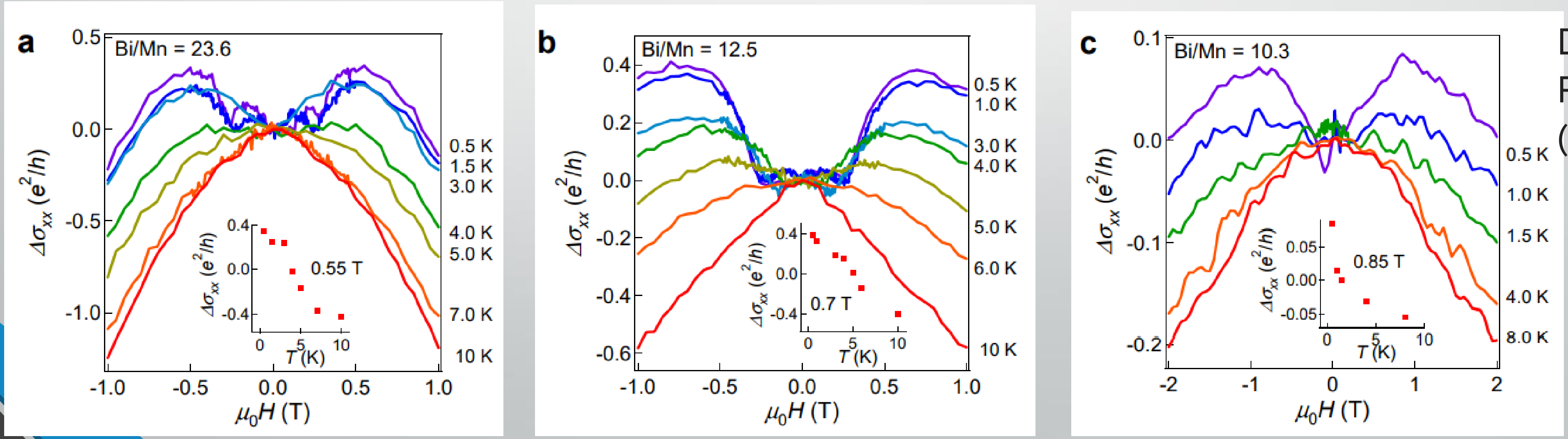

D. Zhang et al., Phys. Rev.B **86** (2012) 205127

Remarks

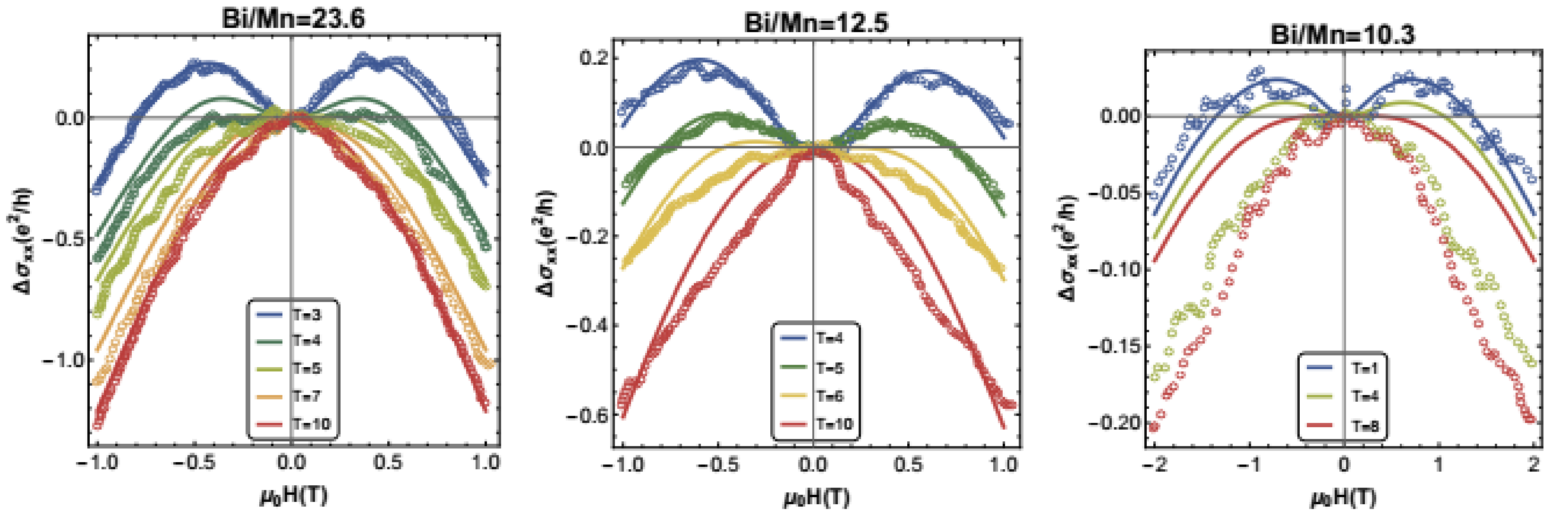

(a) At or near QCP (b) Far from the QCP (c) Farther from the QCP

Among three doping inverse ratio Bi/Mn=23.6, 12.5, 10.6 only the first data could be fit by our theory.

4. Conclusions

- We reported a new black hole solution with hyperscaling violation which is relevant to a magnetic impurity doped quantum materials.
- Finite conductivity and linear in T resistivity can be realized in Lifshitz spacetime without momentum dissipation.
- We calculated all transport coefficients and compare our model with the experimental data.
- We also studied the phase transition from weak localization to weak anti-localization as the critical exponent changes

Outlook

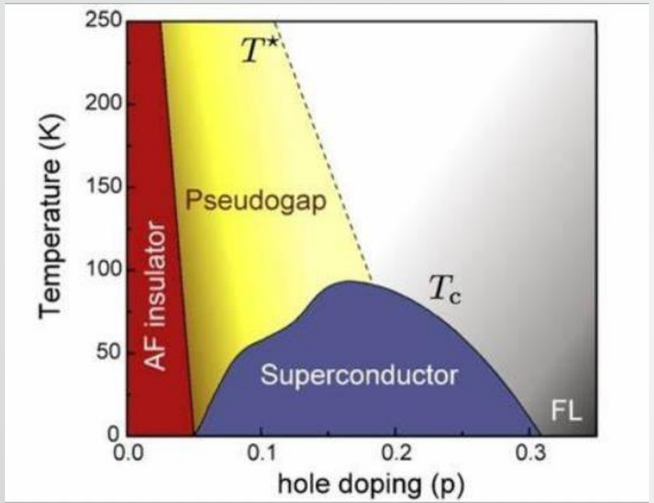

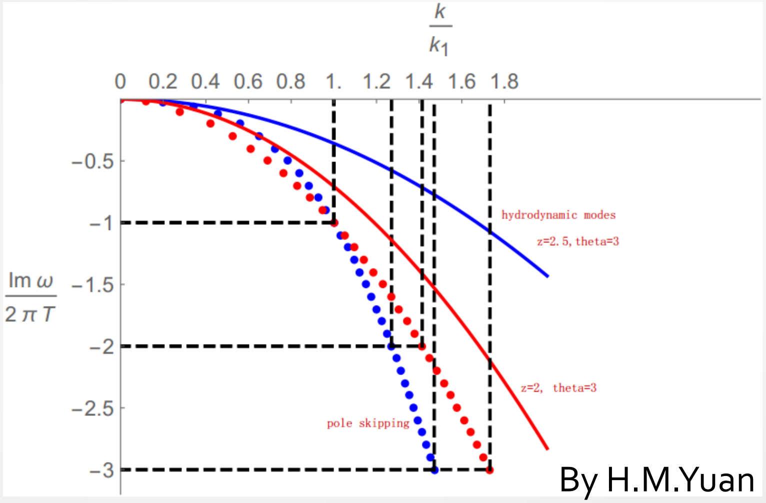

- The superconducting dome for doped Mott insulator with hyperscaling violation

W. Cai, XHG,S. J. Sin (to appear)

- Pole-skipping from holography with hyperscaling violation

H.M. Yuan, XHG, et al (in progress)

Thank You!